applied sciences

MDPI

Article

Mapping Social Vulnerability to Multi-Hazard Scenarios: A GIS-Based Approach at the Census Tract Level

Isabella Lapietra [1], Rosa Colacicco [1,*], Angela Rizzo [1,2] and Domenico Capolongo [1]

[1] Department of Earth and Geoenvironmental Sciences, University of Bari, Via Orabona 4, 70125 Bari, Italy; isabella.lapietra@uniba.it (I.L.); angela.rizzo@uniba.it (A.R.); domenico.capolongo@uniba.it (D.C.)
[2] Interdepartmental Research Centre for Coastal Dynamics, University of Bari, Via Orabona 4, 70125 Bari, Italy
* Correspondence: rosa.colacicco@uniba.it

Abstract: Floods and landslides cause continuous damage to ecosystems, infrastructures, and populations. Particularly, the occurrence and the existence of different natural hazards in the same territory highlight the need to improve risk mitigation strategies for local authorities and community resilience solutions for inhabitants. Analyzing and mapping social vulnerability provides information about the main features of a specific community to deal with natural events. Specifically, the interaction between multi-hazards and the socio-economic environment suggests multidisciplinary assessments that merge the physical and the socio-economic features of the affected territories, providing a useful approach to support multi-risk reduction planning. In this context, the article focuses on integrating landslide and flood hazard scenarios with social vulnerability in the Basilicata Region (southern Italy) at the census tract level. Thirteen municipalities were chosen as multi-hazard hot spots, while open-source platforms were selected for hazard and social vulnerability data collection and analyses. A geographic information system (GIS)-based approach was applied to combine different hazard scenarios with social vulnerability distribution among 1331 census tracts to detect the most vulnerable sub-municipality areas that need special attention in multi-risk reduction strategies. The results are presented in the form of maps, which provide a relevant suitable tool in local emergency planning.

Keywords: social vulnerability; multi-hazard; GIS; multidisciplinary approach; disaster risk reduction

Citation: Lapietra, I.; Colacicco, R.; Rizzo, A.; Capolongo, D. Mapping Social Vulnerability to Multi-Hazard Scenarios: A GIS-Based Approach at the Census Tract Level. *Appl. Sci.* **2024**, *14*, 4503. https://doi.org/10.3390/app14114503

Academic Editors: Wojciech Zgłobicki and Leszek Gawrysiak

Received: 19 April 2024
Revised: 22 May 2024
Accepted: 23 May 2024
Published: 24 May 2024

1. Introduction

Disasters are strictly correlated to the negative effects of significant natural events on the vulnerable elements exposed, which require interdisciplinary analyses for risk reduction strategies. According to the disaster risk reduction (DRR) school of thought, risks result from interactions between the hazard with the exposure and the vulnerability of the affected territory [1]. A hazard is "the potential occurrence of a natural or human-induced physical event or trend or physical impact that may cause loss of life, injury or other health impacts, property damage, social and economic disruption or environmental degradation" [2,3]. Exposure refers to the number of elements (human beings, livelihoods, and assets) located in a hazardous area [1,4]. Vulnerability is the susceptibility of these exposed elements to the impact of a hazard [5]. As disaster risk depends on the severity of the hazard, the number of elements exposed and the susceptibility of these elements to suffering loss and damage, the correlation between natural hazards and the socio-economic conditions of the potentially affected territory implies the necessity of multidisciplinary analyses. In this context, interdisciplinary investigation combines the assessment of the hazard component and evaluates the socio-economic features in terms of exposure and vulnerability.

Natural hazards include floods, ground instabilities, wildfires, typhoons, earthquakes, volcanic activity, extreme temperatures, and drought. Among them, floods and landslides are two of the most dangerous events, as in recent years, both phenomena have occurred regularly as a consequence of heavy rainfall events and deforestation [6], causing continuous damage to ecosystems, infrastructures, and population. Floods occur most commonly

due to heavy rainfall, when natural watercourses lack the capacity to convey excess water, but they can also result from storm surges associated with tropical cyclones, tsunamis, or high tides in coastal areas [7]. Among the hydrological phenomena, various types of floods can be distinguished, such as riverine floods, flash floods, urban floods, and coastal floods. Landslides are "almost all varieties of mass movements on slope including some such as rock falls, topples, and debris flows that involve little or no true sliding" [8], and they are mainly distinguished by rapid (rockfalls, rock avalanches, debris flows, mud flows, rock slides, and soil slides) and slow processes (earth flows, soil slips, rototranslational slides, and rock slides). According to the Emergency Events Database (https://www.emdat.be/ accessed on 10 April 2024), floods have been the most frequently occurring events in Europe (460), with 260 riverine floods, 69 flash floods, 3 coastal floods, and 128 general floods in the last twenty years, causing USD 192,059,583 worth of damage and 2112 deaths. At the same time, nine landslides, eight avalanches, two mudslides and one rockfall have caused damage worth a total of USD 707,837 and 2387 deaths.

Flooding and landslide phenomena are often connected to or coexist in a specific geographic area, producing multi-hazard scenarios. These events, whether concatenated or not, and with no chronological relationship, threaten the same elements at risk in a given geographic area [9]. Generally, multi-hazard contexts include three types of scenarios: aggregate (where hazard events may be unrelated, occurring sequentially in the same location or simultaneously in different locations with concurrent impacts), cascading (events in which one hazard triggers another hazard) and compound (where events are correlated in terms of space and/or time but result from distinct causal pathways [10]).

Due to the complexity of such phenomena, different dimensions of vulnerability (social, physical, environmental, economic, and institutional) need to be taken into account in disaster risk studies. However, a multi-hazard social vulnerability approach represents a significant aid for DRR policy as it provides insights into actions to reduce population vulnerability, improve mitigation, enhance resilience, and promote disaster risk management [11]. Over the past few years, several studies have focused on social vulnerability to multi-hazard scenarios [12–14], especially considering landslide and flood hazards [15–18]. However, only a few studies have been developed in Italy, which is considered the most naturally hazardous area in Europe.

In this study, we implemented a multi-hazard social vulnerability approach at the census tract level considering landslide and flood hazards in the Basilicata Region (southern Italy). We looked at the coexistence of these phenomena in a given geographic area, showing a methodological framework that can be applied to analyze multi-hazard scenarios. The main aim was the development of a cartographic methodology that provides part of the specific risk information useful to construct emergency plans at the local level by using available open data. Indeed, one of the most significant challenges that the scientific community deals with risk analysis is the method of data integration between hazard and vulnerability, as it requires different competences and various types of investigations. For this reason, we integrated two of the main components influencing a multi-risk context by constructing a social vulnerability index (SVI) and relating to with multi-hazard assessment. The present research followed a semi-quantitative and open-data-driven methodology by exploiting the use of a geographic information system (GIS). The social vulnerability assessment was based on a deductive approach [19] that is strictly correlated to a few socio-economic variables available on open platforms at the census tract level and useful to construct a composite index. The choice to work at the census tract (sub-municipality) level is an advantage in risk management strategies and emergency planning, as many studies were developed at the municipality level that were lacking in detailed socio-economic information. The cartographic outputs presented in this study offer valuable instruments for civil protection agencies, facilitating precise identification of areas with heightened vulnerability within the possible affected territories. Moreover, one of the novelties of this research is linked to the use of open national hazard data that have never been used to investigate specific multi-hazard context at the local level.

The structure of the manuscript is organized as follows: Section Multi-Hazard Context in the Basilicata Region presents an overview of the multi-hazard context within the Basilicata region. Section 2 delineates the analytical framework employed in this research. Section 3 is dedicated to presenting the outcomes associated with the multi-hazard assessment, the evaluation of social vulnerability, and the synthesis of hazard and vulnerability findings. Section 4 offers a critical examination of these results. The manuscript concludes with a discussion of limitations and proposes directions for future research.

Multi-Hazard Context in the Basilicata Region

The Basilicata Region (40°38′35.077″ N 15°58′11.957″ E) is located in southern Italy (Figure 1) and covers a total area of 10,073 km^2, including 131 municipalities and hosting 578,036 inhabitants, 187,254 buildings, 30,043 enterprises and 2028 cultural heritages (https://idrogeo.isprambiente.it/app/pir/r/17, accessed on 19 March 2023). The region is one of the most hazard-prone areas of the Italian territory, as nearly 50% of Basilicata towns are exposed to a high risk of landslides or floods [20]. Basilicata is known for its high frequency of extreme hydrogeological events as several landslides and floods have extensively affected the region because of its geological characteristics and the dynamics of precipitation producing extensive damage to urban areas and infrastructures [21]. According to Lazzari and Piccarreta [22], the region has the highest density of landslides, with more than 27 landslide areas every 100 km^2, mostly related to predisposing conditions, such as prevailing clay materials [23], the morphological setting of the slopes, and conditions concerning extreme rainfall events or human activity. Moreover, the region has been affected by recurrent flooding events, not exceptionally intense on an absolute scale [24], which have caused significant economic damage to infrastructures, agricultural and tourist activities, and archeological heritage. Examples of significant events with a declared state of emergency that occurred in the Basilicata Region in the last ten years are listed in Table 1. These events led the scientific community to develop relevant research for landslide characterization [20,22,25,26] and flood monitoring, vulnerability and risk mapping [24,27–33].

In terms of national and regional hazard data, Figure 1 shows the spatial distribution of the landslide and flood hazard in the Basilicata Region, derived from Italian Institute for Environmental Research and Protection (ISPRA) 2020–2021 mosaic layers. The national mosaics of landslide and flood hazards are created by ISPRA on the basis of the data provided by the District Basin Authorities and are related to the Hydrogeological Management Plan (PAI), which aims toward soil conservation, defense, and valorization in the areas at risk due to geomorphological processes.

Table 1. List of major flood and landslide events that have occurred in the past ten years. Data were collected from Emergenza Basilicata, Protezione Civile (http://www.emergenza.regione.basilicata.it/emerg_alluv_2011/section.jsp?sec=100215, accessed on 20 March 2023).

Event	Time Period	Location
Flood	7–8 October 2013	Municipality of Bernalda, Montescaglioso, Pisticci, Scanzano Jonico
Flood	1–3 December 2013	Several municipalities located in Matera and Potenza province
Landslide	3 December 2013	Municipality of Montescaglioso
Landslide	Triggered in February 2014 and declaration of the state of emergency in December 2017	Municipality of Stigliano
Landslide	29 January 2019	Municipality of Pomarico
Flood	11–12 November 2019	Basilicata Region

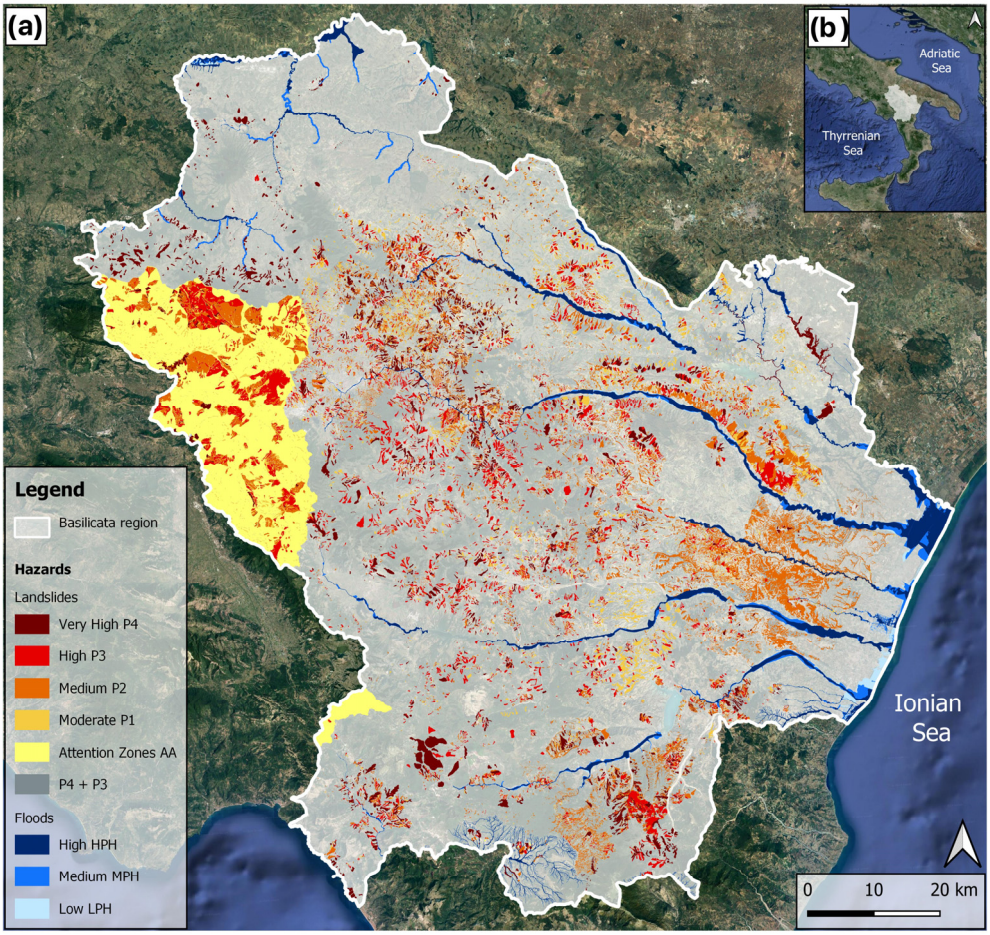

Figure 1. (**a**) Spatial distribution of landslide and flood hazard in the Basilicata Region (the attention areas (AA) correspond to portions of the territory characterized by possible instability to which no hazard class has yet been associated [34]); (**b**) geographic location of the Basilicata Region within the national context. Data were collected from the IdroGEO website (https://idrogeo.isprambiente.it/app/page/open-data, accessed on 20 March 2024). Basemap: Google Satellite.

In the case of flood hazards, the informative layer defines the extension of the floodable areas for each of the probability scenarios envisaged in art. 6 of the European Union Floods Directive (2007/60/EC): High-Probability Hazard (HPH—a high probability of floods); Medium-Probability Hazard (MPH—a medium probability of floods); Low-Probability Hazard (LPH—a low probability of floods). According to Legislative Decree 49/2010, these scenarios correspond to the areas that can be flooded following flood events, with return periods between 20 and 50 years (HPH—high probability of or frequent floods), between 100 and 200 years (MPH—medium probability of or infrequent floods), and with a return period exceeding 200 years (LPH—low probability of extreme event scenarios).

Concerning the landslide hazard, the informative layer contains information about landslides that have already occurred and the portion of territories potentially susceptible to new landslide events [34]. In this case, the landslide hazard classification is distinguished into four main classes (P1, P2, P3, and P4) on the basis of interventions that can be implemented. According to ISPRA [34], class P4 covers areas characterized by a "very high landslide hazard" (P4), where building demolition and vulnerability reduction, mass movement reclamation, and maintenance of mass movement areas are permitted. In areas classified as having a "high landslide hazard" (P3), in addition to the interventions included in P4 areas, expansion interventions in existing buildings for hygienic–sanitary adaptation and the construction of new waste treatment plants are generally considered. In areas classified as having a "medium landslide hazard" (P2), the interventions are those provided

via territorial and urban planning and are generally subject to safety checking for instability conditions and geomorphological process changes. Finally, in areas classified as having a "moderate landslide hazard" (P1), any type of general intervention envisaged via territorial and urban planning is authorized.

More detailed information about the national landslide inventory and the kinematics linked to these events can be found in the IFFI project (https://idrogeo.isprambiente.it/app/iffi/r/17?@=40.520557401702234,16.101003400000003,5, accessed on 20 March 2024), whereas regional data can be collected from the landslide inventory map created by Lazzari et al. [20].

The delimitation of flood and landslide hazard areas has led to the calculation of exposure indicators (2021), which are shown in Table 2, with a general focus on the multi-hazard context in the Basilicata region.

Table 2. Exposure data linked to flood and landslide hazards. Data were collected from the Idro-Geo website (https://idrogeo.isprambiente.it/app/pir/r/17, accessed on 20 March 2024) to give information about the inventory of elements exposed to multi-hazard conditions.

Hazard Type	Class	Territory (km^2)	Population (%)	Household (%)	Buildings (%)	Business (%)	Cultural Heritage (%)
Flood	HPH	264.06	0.7	0.7	1	0.8	2.8
	MPH	349.25	1.1	1.1	1.4	1.3	2.9
	LPH	378.91	1.2	1.2	1.5	1.5	3.1
Landslide	P4	268.07	3.3	3.4	4.3	2.9	8.3
	P3	334.23	3.7	3.9	4.4	3.7	4.8
	P2	549.82	4.4	4.5	5	4.2	5
	P1	212.35	2.4	2.4	2.5	2.4	3

2. Materials and Methods

A GIS-based approach was applied to conduct a multidisciplinary analysis based on three main operational steps: a multi-hazard assessment, a social vulnerability evaluation, and the combination of the results. The investigation was carried out with an open-data-driven and semi-quantitative approach at the census tract level. The semi-quantitative approach allowed us to combine results derived from the different types of analyses (qualitative and quantitative) in a single classification, providing an overview of the main findings. As regards the data used, the ISPRA dataset was selected to collect hazard data (Section Multi-Hazard Context in the Basilicata Region), the ISTAT open platform was used to extract geographic and administrative boundaries (https://www.istat.it/it/archivio/104317#accordions, accessed on 6 March 2024), with census socio-economic data (https://www.istat.it/it/archivio/285267, accessed on 6 March 2024), and the repository of the Department of Civil Protection (DCP) was consulted for building data (https://github.com/pcm-dpc/DPC-Aggregati-Strutturali-ITF-Sud/tree/master/Sud/Basilicata/Matera, accessed on 6 March 2024). All the data collected from these sources refer to the year 2021, while the cartographic bases refer to 2011.

Figure 2 depicts the methodological workflow that, starting from the selection of the municipalities to be investigated, leads to the integration process at the census tract level through GIS-based analysis. Almost all the steps represented in Figure 2 were carried out via the use of GIS a part from the social vulnerability evaluation, which was based on a mathematical operation (Section 2.2). Currently, the census tract level represents the smallest statistical area at the sub-municipality level in Italy and can be useful for building high-resolution maps for risk management strategies.

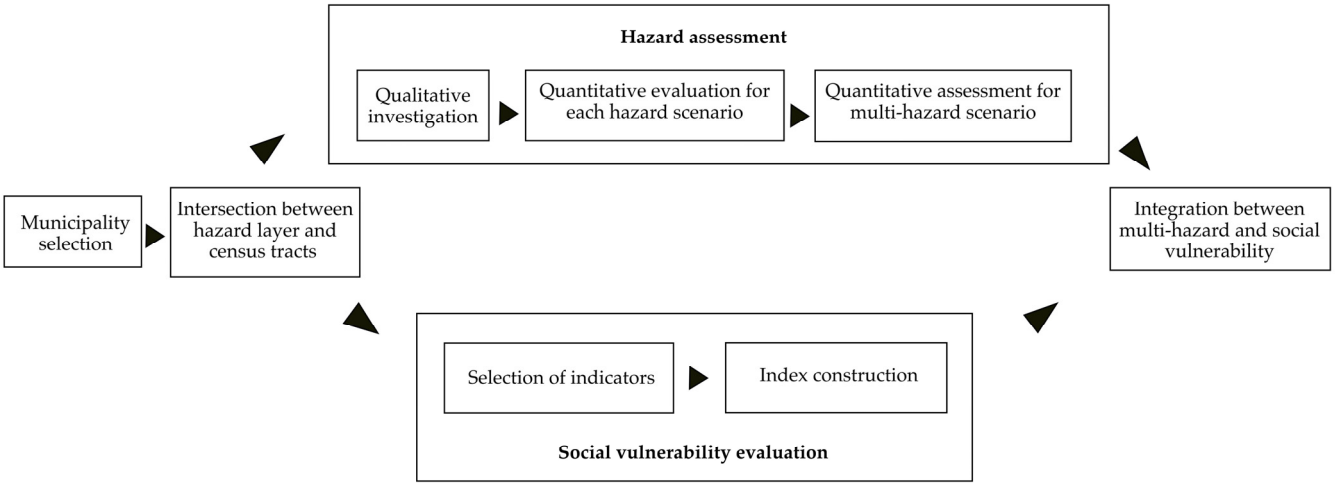

Figure 2. Methodological workflow for data integration at census tract level.

2.1. Study Area Selection and Hazard Assessment

After an extensive literature search focused on the hazard context in the Basilicata Region (Section Multi-Hazard Context in the Basilicata Region), the municipalities choice was based on the results obtained via the flood hazard mapping performed in previous works [31] coupled with the neighboring municipalities affected by significant landslide events in the past (Section Multi-Hazard Context in the Basilicata Region) and intersected by the landslide hazard layer in GIS environment (Figure 1). In particular, the intersection tool allowed us to conduct both qualitative and quantitative investigations based on the percentage of the territory potentially affected by landslide, flood, and multi-hazard scenarios for each census tract. The cartographic methodology was specifically explained in Lapietra et al. [31]. However, the landslide hazard layer was also included in this analysis in order to construct a multi-hazard map.

As regards the qualitative investigation, a specific hazard classification was provided to show the combination of different hazard types found within each census tract (Table 3). As shown in Table 3, the column "Scenario" includes a set of alphanumeric codes derived from the specific hazard classes provided in Section Multi-Hazard Context in the Basilicata Region. Census tracts only intersected by the landslide hazard layer fell into the LH (landslide hazard) classification, census tracts only characterized by flood hazard were related to the FH (flood hazard) classification, whereas census tracts potentially affected by both hazards were associated with the MH (multi-hazard) scenario. Therefore, the letters included in each scenario provide the type of hazards located in each census tract, whereas the numbers represent the count of the combinations. In total, 13 scenarios were detected in census tracts only affected by LHs, 3 scenarios were detected for the case of FHs and 15 scenarios were detected for census tracts intersected by MHs. The advantage of this qualitative methodology is that is provides specific hazard information for each census tract, avoiding cartographic overlap in the final maps.

In terms of quantitative analysis, the percentage of the territory potentially affected was determined by calculating the extent of the LPH, MPH, HPH, P1, P2, P3, and P4 scenarios, in km^2, in each census tract. Since P1, P2, P3, and P4 (Section Multi-Hazard Context in the Basilicata Region) covered different areas within a single census tract, each extent was summed up to obtain a unique value for the LH scenario. On the contrary, since the LPH flood scenario often included census tract areas characterized by MPH and HPH, the extent of each scenario was treated separately in order to preserve the different return period scenarios.

Table 3. Codification process for multi-hazard qualitative analysis. The "Hazard type" column represents the type of hazard combination found within each of the census tracts. Each combination is summarized in the "Scenario" column. LH codes (green color) are associated with census tracts only intersected by landslide hazards, FH codes (blue color) are associated with those only intersected by flood hazards, and MH codes (violet color) are associated with those affected by floods and landslides and falling in multi-hazard scenarios.

Landslide		Flood		Multi-Hazard	
Hazard_Type	**Scenario**	**Hazard_Type**	**Scenario**	**Hazard_Type**	**Scenario**
P1	LH1	LPH	FH1	MPH LPH P1 P2	MH1
P2	LH2	MPH HPH	FH2	MPH LPH P2 P3	MH2
P3	LH3	HPH MPH LPH	FH3	MPH LPH P1 P2 P3 P4	MH3
P4	LH4			HPH MPH LPH P1	MH4
P1 P2	LH5			HPH MPH LPH P2	MH5
P1 P3	LH6			HPH MPH LPH P3	MH6
P2 P3	LH7			HPH MPH LPH P4	MH7
P2 P4	LH8			HPH MPH LPH P1 P2	MH8
P3 P4	LH9			HPH MPH LPH P2 P3	MH9
P1 P2 P3	LH10			HPH MPH LPH P2 P4	MH10
P1 P2 P4	LH11			HPH MPH LPH P1 P2 P3	MH11
P2 P3 P4	LH12			HPH MPH LPH P1 P2 P4	MH12
P1 P2 P3 P4	LH13			HPH MPH LPH P2 P3 P4	MH13
				HPH MPH LPH P1 P2 P3 P4	MH14
				MPH LPH P2	MH15

The extent of each scenario was then compared with the total extent of the census tracts in order to measure the percentage of the territory potentially affected by LH, HPH, MPH, and LPH. The percentage of the territory affected ranged between 0% and 100%. Census tracts with no part of the territory affected were excluded from the classification, whereas the others were classified into five hazard levels: Level 1 (very low), Level 2 (low), Level 3 (medium), Level 4 (high), and Level 5 (very high). This type of analysis led us to build a single-hazard map for the LH and FH scenarios. Moreover, in order to include census tracts affected by the multi-hazard scenario, a hazard matrix (Figure 3) was constructed to combine different hazard classes through the use of the raster calculator in the GIS environment.

Hazard_matrix (FH+LH)		LH_class				
		1	2	3	4	5
FH_class	1	2	3	4	5	6
	2	3	4	5	6	7
	3	4	5	6	7	8
	4	5	6	7	8	9
	5	6	7	8	9	10

Figure 3. Hazard matrix applied for quantitative multi-hazard analysis.

2.2. Social Vulnerability Evaluation and Hazard Integration

Since this work was based upon an open data-driven approach, the identification of socio-economic indicators was facilitated by the availability of the socio-economic variables already provided by ISTAT at the census tract level and the building data from DPC. Within the ISTAT dataset and according to the literature, 9 variables that play a crucial role in incrementing social vulnerability were chosen to construct the composite index. Table 4 shows the indicator list with the relative proxy variables used for the social vulnerability analysis. Each variable corresponds to a specific value explained in the "Description"

column, whereas information about indicators and variables can be found in the papers listed in "Reference". This column represents the justification of the variables chosen for this investigation.

Table 4. Selection of indicators that influence social vulnerability. The variables were extracted from the open dataset ISTAT's available at the census tract level.

Indicator	Variable	Description	References
Population density	Pop_density	Number of inhabitants/km^2	[35–41]
Build up density	Build_density	Number of buildings/km^2	[37,42,43]
Age	Eld	% of inhabitants with age > 65	[16,44,45]
	Child	% of inhabitants with age < 15	[43,46]
Gender	Wom	% of women residents	[34,44,47]
Education	Low_ed	% of illiterate residents or with low education	[38,47–49]
Employment	Unemp	% of unemployed residents	[38,50–52]
Foreign	For	% of foreign people	[16,39,47,53]
Household	House6+	% of households with 6 or more family members	[54,55]

Once the variables were standardized, they were aggregated to provide a unique number score for each census tract through Equation (1):

$$SVI = \Sigma(Pop\_dens, Build\_dens, Eld, Child, Wom, Low\_ed, Unemp, For, House6+) \quad (1)$$

where SVI represents the social vulnerability index and the equation components refer to the variables explained in Table 1. The results obtained were then classified into five classes (Class 1 = very low social vulnerability; Class 2 = low social vulnerability; Class 3 = medium social vulnerability; Class 4 = high social vulnerability; and Class 5 = very high social vulnerability) and distributed through GIS spatial analysis tools.

As a final step, the different hazard levels were combined with SVI classes through a GIS-based raster analysis tool to obtain the final map. The raster analysis was conducted by using the risk formula provided in Section 1, and the census tracts were spatially distributed between low and high levels.

3. Results

3.1. Municipality Selection

The flood hazard map provided by Lapietra et al. [31] detects the municipalities located on the Ionian coast as the most exposed to flood hazard in the case of the LPH scenario. These municipalities are Bernalda, Pisticci, Scanzano Jonico, Policoro, Rotondella, and Nova Siri. In order to include municipalities intersected by the landslide hazard layer (Figure 1) and affected by past significant events (Section Multi-Hazard Context in the Basilicata Region), seven neighboring municipalities were also selected: Montescaglioso, Pomarico, Craco, Montalbano Jonico, Tursi, Colobraro, and Valsinni. As shown in Figure 4 and Table 5, thirteen municipalities in total were identified for the investigation. In particular, the study area is characterized by 1391.95 km^2 and 1331 census tracts.

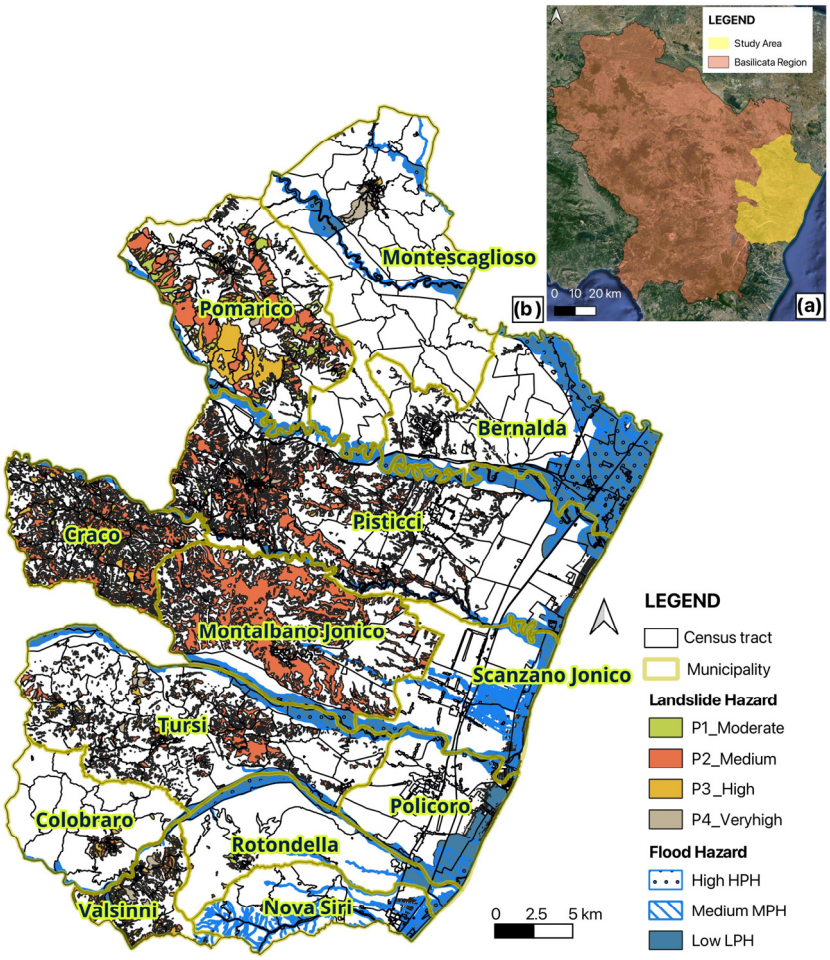

Figure 4. Maps showing the geographic location of the study area (yellow color) within the regional context (**a**) and an indication of the municipalities and the census tracts affected by flood and landslide hazards (**b**). Basemap: Google Satellite.

Table 5. Table showing the 13 municipalities belonging to the study area with the number of inhabitants registered in 2021 and the number of census tracts.

Municipality	Population 2021 (N.)	Census Tract (N.)
Bernalda	11,964	179
Colobraro	1070	42
Craco	644	51
Montalbano Jonico	6.796	59
Montecaglioso	9.247	108
Nova Siri	6.708	87
Pisticci	16.836	305
Policoro	17.685	148
Pomarico	3.832	86
Rotondella	2.448	44
Scanzano Jonico	7.525	96
Tursi	4.753	93
Valsinni	1.373	33

3.2. Hazard Assessment

3.2.1. Qualitative Evaluation

The qualitative hazard distribution highlights the presence of 755 census tracts characterized by single hazard (flood or landslide) and 127 covered by multi-hazard (MH)

sectors (flood + landslide). Apart from Policoro, all municipalities are characterized by single-hazard and MH scenarios.

In the first case, 470 census tracts are intersected by flood hazard (FH), mostly located within the Ionian coast in the municipalities of Bernalda, Pisticci, Scanzano Jonico, Policoro, Rotondella, and Nova Siri (Figures 5 and 6), and along the Bradano river within the municipality of Montescaglioso (Figure 6b). On the contrary, 287 census tracts are affected by landslide hazard (LH) in the municipalities of Tursi, Pisticci, Pomarico, Montescaglioso, Montalbano Jonico, and Craco (Figure 5). An extended territory characterized by the MH scenario is located in the central and southern sectors of the study area across the municipalities of Pisticci, Montalbano Jonico, Scanzano Jonico, Tursi, Rotondella, Nova Siri, Colobraro, and Valsinni (Figure 6c,d).

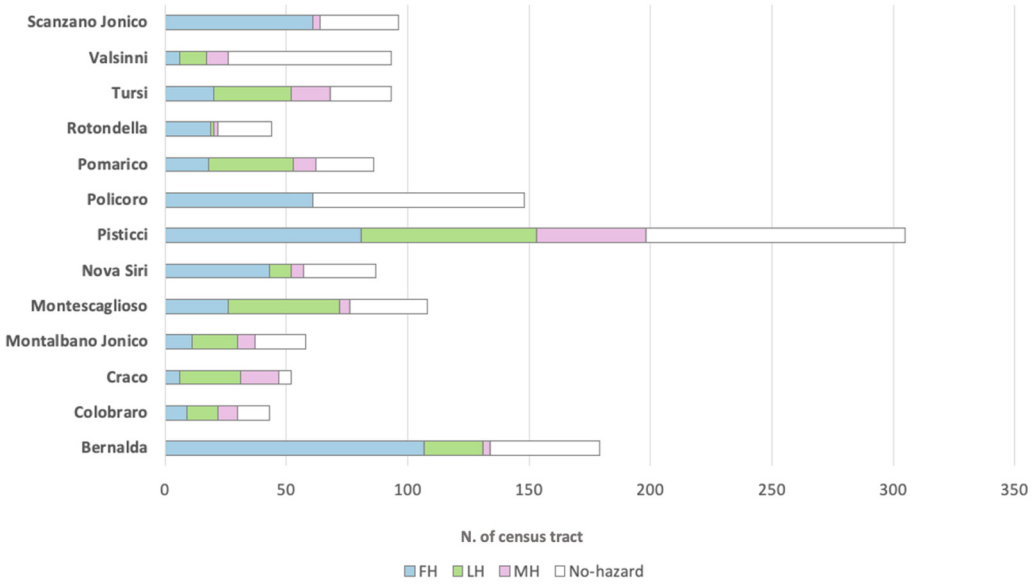

Figure 5. Histogram showing the number of census tracts intersected by flood hazard (FH), landslide hazard (LH), and multi-hazard (MH) for each municipality under investigation.

According to Figures 5 and 6, almost all census tracts belonging to the FH scenario are associated with FH3 (417), whereas 31 census tracts are related to FH2 and 22 are related to FH1, especially in the municipality of Policoro (Figure 6d). As shown in Figure 6, scenarios with more variety are highlighted in census tracts affected by LH and MH. Starting from the northern sector (Figure 6c), the central part of Montescaglioso, where the town center is located, is represented by 47 census tracts classified as having LH with scenarios corresponding to LH3, LH4, LH5, LH8, LH9, and LH12, whereas 5 census tracts, located in the north-eastern part of the municipality, are characterized by them H4, MH7, MH9, MH10, and MH12 scenarios. Along the border with this municipality, Bernalda only shows 2 census tracts associated with MH (MH5 and MH8), while it shows 34 census tracts associated with LH2, LH4, LH5, LH7, LH8, and LH12, also corresponding to the town center. In the municipality of Pomarico, 34 census tracts are found in LH2, LH3 LH4, LH5, LH7, LH9, LH10, LH11, LH12, and LH13 scenarios, while 9 census tracts fall in MH5, MH9, MH11, MH13, and MH14 scenarios. The town center is also located in an LH area in this case. Moving to the central sector of the study area (Figure 6c), 68 census tracts are covered by LH1, LH2, LH3, LH4, LH5, LH8, LH11, and LH13 scenarios, and 46 are covered by the MH4, MH5, MH8, and MH14 hazard combinations within the municipality of Pisticci. Most of the census tracts located in the municipality of Craco (25) are intersected by LH2, LH3, LH4, LH5, LH7, LH9, LH10, LH11, LH12, and LH13 scenarios, whereas 15 census tracts are characterized by MH5, MH8, MH9, and MH11 scenarios. The municipality of Montalbano Jonico is represented by 19 census tracts in LH2, LH5, LH7, LH8, and LH12 scenarios, including the town center, and 8 census tracts in the MH4, MH5, MH8, MH11,

and MH14 hazard combinations. Moving towards the south, Scanzano Jonico shows only three census tracts located in MH5 scenario, bordering Montalbano Jonico.

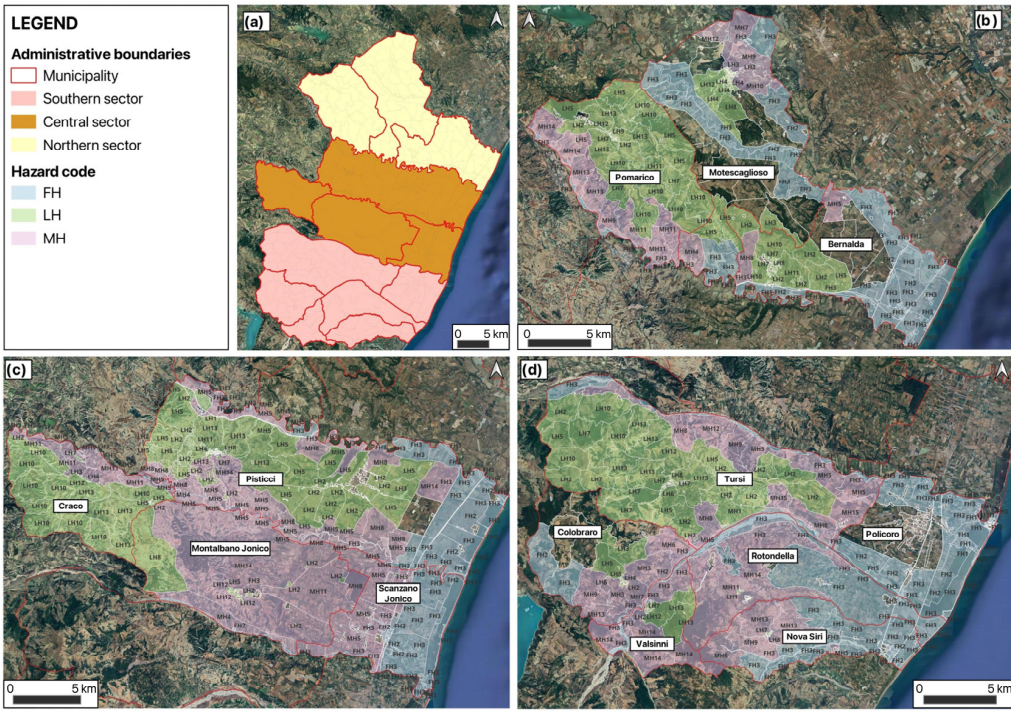

Figure 6. Hazard qualitative distribution derived from the codification process (Table 1) in different study area sectors (**a**) at the census tract level. Magnified view of the northern (**b**), central (**c**), and southern sector (**d**). FH = flood hazard; LH = landslide hazard; MH = multi-hazard. The white lines represent the census tract boundaries. Basemap: Google Satellite.

Lastly, within the southern sector (Figure 6d), the municipality of Tursi is represented by 33 census tracts in the LH2, LH4, LH5, LH6, LH7, LH8, LH9, LH10, LH12, and LH13 scenarios (including the city town area) and 13 census tracts belonging to MH1, MH5, MH8, MH9, MH12, and MH15; Colobraro shows 12 census tracts related to LH2, LH3, LH4, LH5, LH6, LH7, LH8, and LH12 and 9 census tracts related to MH3, MH6, MH7, MH9, MH10, and MH13; Valsinni is characterized by 11 census tracts falling into LH2, LH7, LH12, and LH13 and 9 census tracts corresponding to MH7, MH10, MH13, and MH14; Rotondella is represented by one census tract associated with LH1 and two census tracts associated with MH11 and MH14 scenarios; Nova Siri has three census tracts intersected by the LH4, LH7, and LH12 landslide hazard combinations and six census tracts characterized by the MH5, MH9, and MH13 scenarios.

As shown in the qualitative investigation and looking at the hazard spatial distribution, the central and southern sector of the study area is the most exposed to multi-hazard scenarios.

3.2.2. Quantitative Investigation

The hazard quantitative assessment results in four hazard maps showing the single-hazard classification at the census tract level (Figure 7) based on the percentage of the territory potentially affected by LH and FH (HPH, MPH, and LPH). In the case of the LH scenario (Figure 7a), 32 census tracts fall in the very-high-hazard class (Level 5), 25 fall in the high-hazard class (Level 4), and 45 fall in the medium-hazard class (Level 3), mostly included in the municipalities of Pomarico, Pisticci (northern area), Craco, Montalbano Jonico, Colobraro, Valsinni, and Nova Siri. In total, 65 census tracts are associated with the low-hazard class (Level 2), whereas 231 are related to the very-low-hazard class (Level 1), spatially distributed across all the municipalities apart from Policoro. As a main result

of landslide hazard quantitative analysis, the central sector of the study area (Figure 6a) coupled with the municipalities of Pomarico and Valsinni are the most exposed to LH.

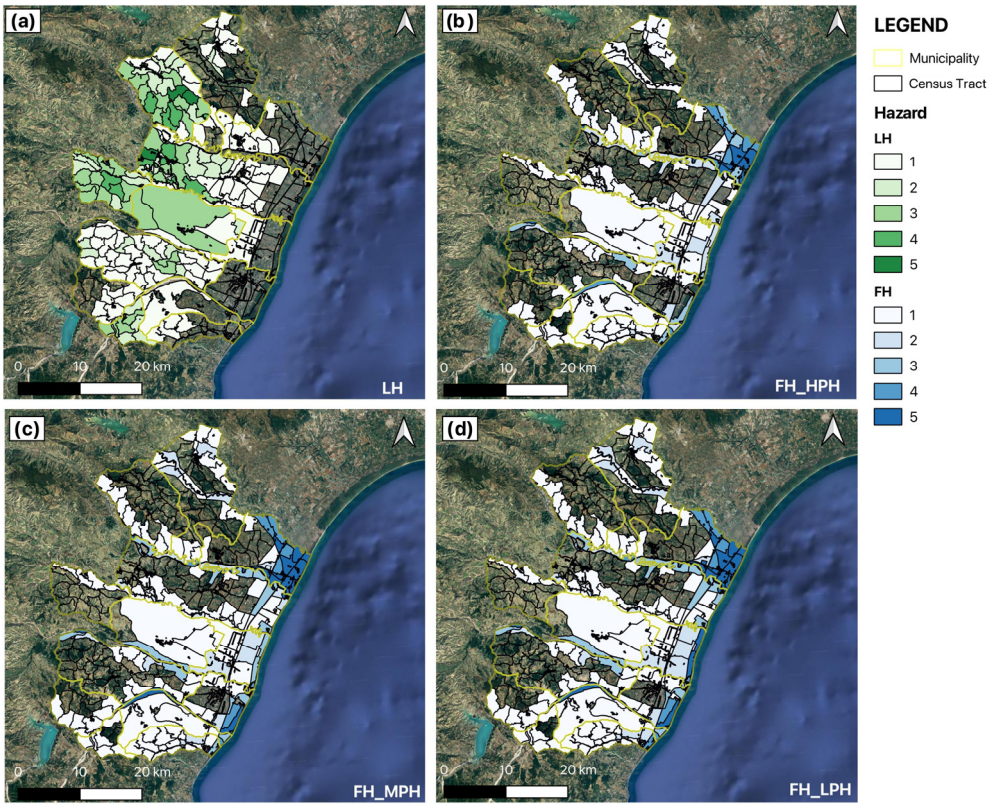

Figure 7. Classification of the census tracts based on the percentage of the territory affected by landslide hazard (**a**) and flood hazard in the high- (**b**), medium- (**c**), and low (**d**)-probability hazard scenarios. The numbers are classified as follows: 1 = very low; 2 = low; 3 = medium, 4 = high; 5 = very high. Basemap: Google Satellite.

According to Figure 7b–d, all the municipalities intersected by FH show similar characteristics in the case of LPH, MPH, and LPH scenarios in terms of spatial distribution. The slight difference between these scenarios is the increments of the flood hazard classes from HPH to MPH and LPH in some census tracts mostly located on the Ionian coast. The municipalities of Bernalda, Scanzano Jonico, Pisticci, Policoro, and Nova Siri show the highest number of census tracts (296) and therefore represent the maximum percentage of the territory potentially affected by FH (Classes 4 and 5) in the case of HPH, MPH, and LPH.

Figure 8 depicts the main outcome of the multi-hazard investigation, derived from the overlap between LH and FH (LPH, MPH, and HPH) scenarios. In this case, the spatial distribution of census tracts affected by multi-hazards is similar. Table 6 represents an example of the results derived from the application of the multi-hazard matrix (Section 2.1), showing the number of census tracts exposed to different multi-hazard classes in the case of LH + FH in the MPH scenario. Moreover, information about the qualitative multi-hazard classification is also provided to give information about the specific multi-hazard associated with the different classes. As a result, the majority of census tracts fall in low-multi-hazard classes (77), 7 census tracts belong to the medium multi-hazard level, and 23 are classified as having high multi-hazard. The municipalities with the highest number of census tracts affected by multi-hazard are Pisticci and Tursi. However, Pisticci shows the highest level of multi-hazard exposure.

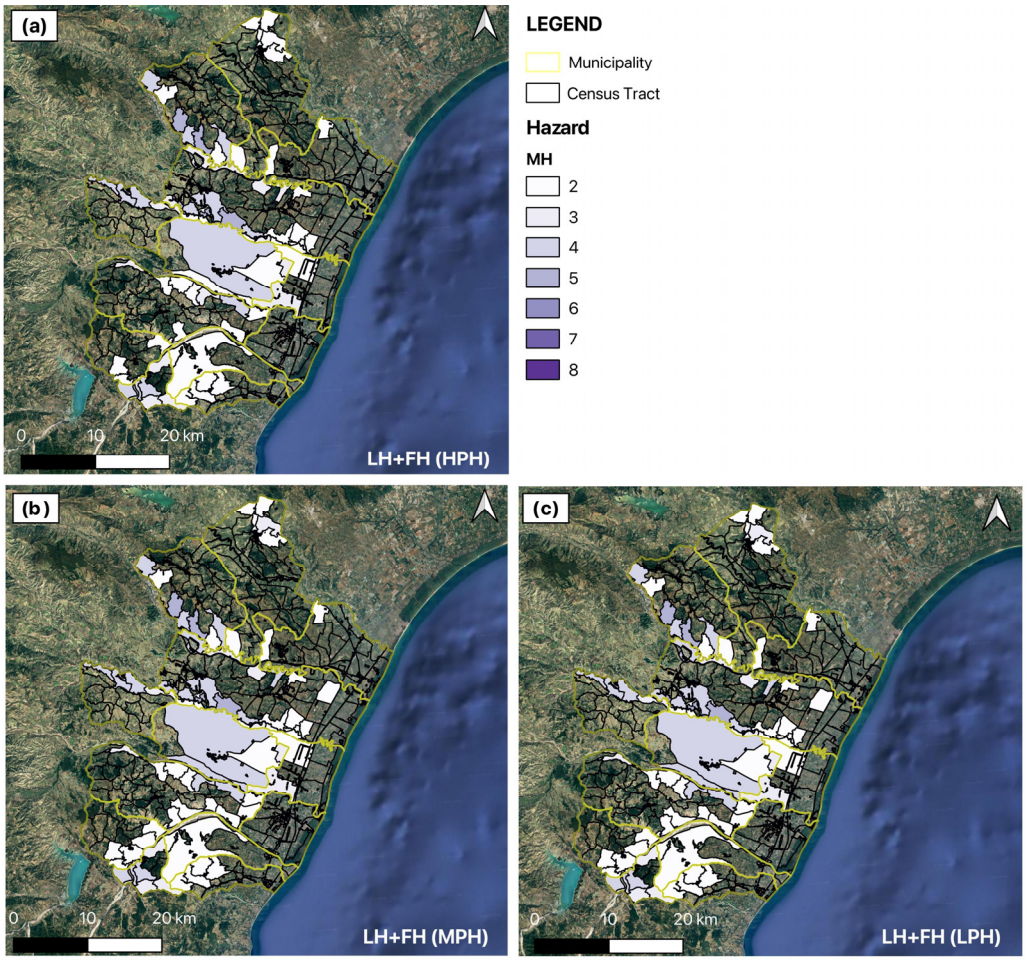

Figure 8. Classification of the census tracts affected by multi-hazards, derived from the overlap between the landslide hazard layer (LH) and the flood hazard layer (FH) in high- (**a**), medium- (**b**), and low- (**c**) probability hazard scenarios. The class ranges between 2 (very, very low) and 8 (very, very high). Basemap: Google Satellite.

3.3. Social Vulnerability Evaluation

According to Section 2.2, the socio-economic variables were aggregated trough Equation (1) to obtain a "synthetic" score for each census tract and to evaluate the SVI. In Figure 9, the spatial distribution of the SVI is provided, whereas Figure 10 depicts the social vulnerability context in each municipality under investigation. Looking at the general distribution of social vulnerability classes in the study area, most of the census tracts fall into Class 1 (N. = 899), showing a very low SVI, followed by Class 3 (medium level, N. = 181), Class 4 (high level, N. = 154), Class 2 (low level, N. = 84) and Class 5 (very high level, N. = 13). A similar trend is depicted in each municipality, where Class 1 of SVI represents the majority of socio-economic conditions at census tract level succeeded by medium and high classes of the SVI (Classes 3 and 4), especially in relation to census tracts located in town centers areas (Figure 9, yellow circle). As shown in Figure 10, most of the census tracts fall into the class with very low social vulnerability; however, Bernalda, Pisticci, Motescaglioso, Montalbano Jonico, Scanzano Jonico, Policoro, Colobraro, Rotondella, Tursi, Valsinni, and Nova Siri show extended territories affected by medium, high, and very high social vulnerability.

Table 6. Table showing the number of census tracts exposed to different multi-hazard classes in the case of LH + FH (MPH) for each municipality affected by MH. The columns related to "MH Code" show the type of multi-hazard derived from the qualitative investigation for each semi-quantitative level. The shades of violet represent the different levels of multi-hazard, in correlation with Figure 8.

Municipality	Low MH (Class 2–4)	MH Code	Medium MH (Class 5)	MH Code	High MH (Class 6–8)	MH Code
BERNALDA	2	MH5, MH8	0		0	
COLOBRARO	5	MH3, MH6, MH9, MH13	0		3	MH7, MH10
CRACO	6	MH5, MH9, MH11	0		7	MH5, MH8, MH9
MONTALBANO JONICO	4	MH4, MH8, MH11, MH14	0		3	MH5
MONTESCAGLIO	5	MH4, MH7, MH9, MH10, MH12	0		0	
NOVA SIRI	4	MH5, MH9, MH13	0		0	
PISTICCI	20	MH5, MH8, MH14	3	MH5, MH8, MH14	19	MH4, MH5, MH8,
POMARICO	5	MH9, MH11, MH14	2	MH11, MH13	1	MH5
ROTONDELLA	2	MH11, MH14				
SCANZANO JONICO	2	MH5	0		0	
TURSI	17	MH1, MH5, MH8, MH9, MH12, MH14, MH15,	0		1	MH5
VALSINNI	5	MH14	2	MH7, MH10	2	MH7, MH13

3.4. Integration between Social Vulnerability, Single-Hazard, and Multi-Hazard Classes

As a final result, Figure 11 represents the outcomes derived from the combination of SVI classes (Figure 9) and hazard classes (Figures 7 and 8) at the3 census tract level. In particular, the maps provide information about the product between LH and SVI (green scale), FH and SVI (blue scale), and MH and SVI (violet scale). Census tracts falling in the green scale represent areas with different levels of social vulnerability only exposed to different levels of landslide hazard, census tracts related to the blue scale outline areas with different levels of social vulnerability only exposed to different levels of flood hazard, and census tracts associated corresponding to the violet scale show areas with different levels of social vulnerability exposed to different levels of multi-hazard (flood and landslide). The details of this type of classification are presented in Table 4, where quantitative and qualitative information derived from the entire analysis are provided for each municipality.

Looking at the general final map (Figure 11) and Table 7, 14 census tracts correspond with the population with the high class of social vulnerability to landslide hazards in the municipalities of Craco, Montescaglioso, Pisticci, and Tursi; 16 census tracts are related to flood hazards in the municipality of Bernalda and Nova Siri; 6 census tracts fall in the multi-hazard context within the municipality of Craco, Montalbano Jonico, Montescaglioso, and Pisticci.

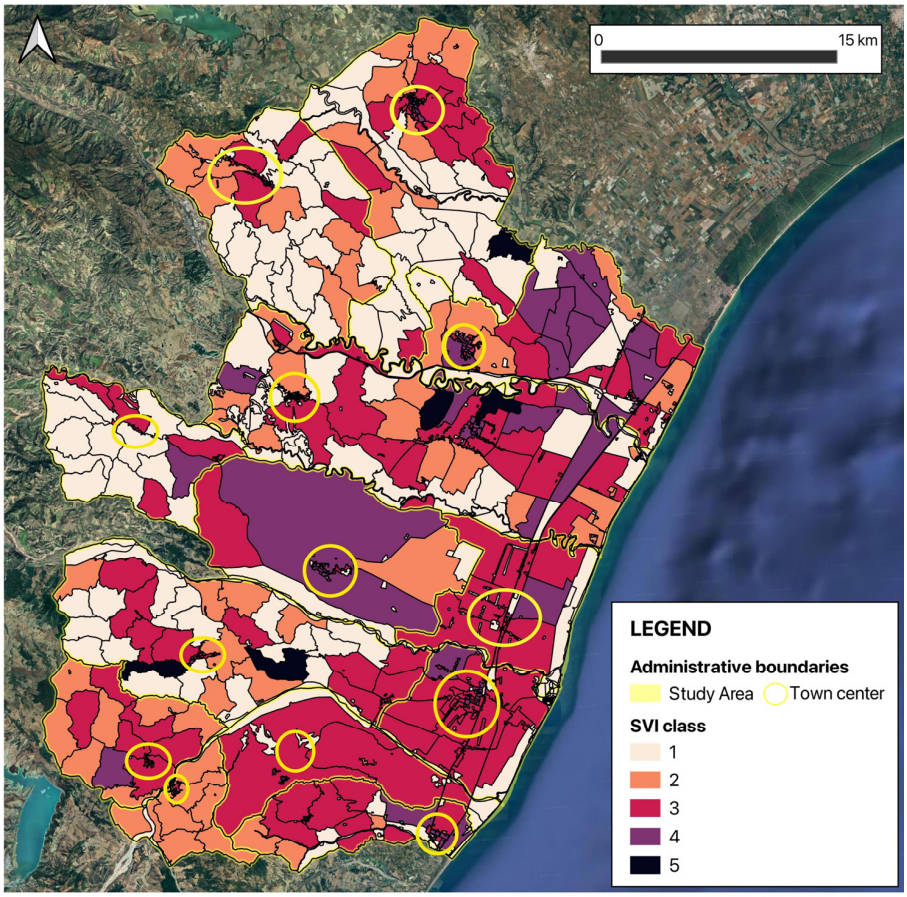

Figure 9. Spatial distribution of the SVI class based on eq.1 at the census tract level: 1 = very low social vulnerability; 2 = low social vulnerability; 3 = medium social vulnerability; 4 = high social vulnerability; 5 = very high social vulnerability. Basemap: Google Satellite.

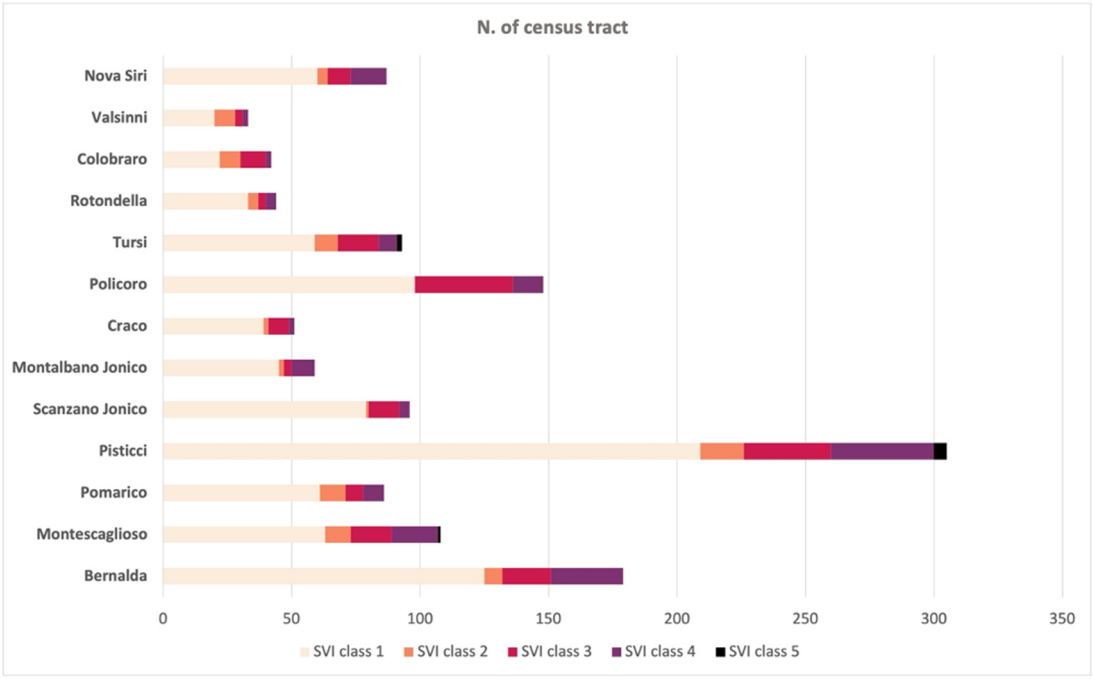

Figure 10. Histogram showing the number of census tracts with their relative levels of social vulnerability for each municipality under investigation.

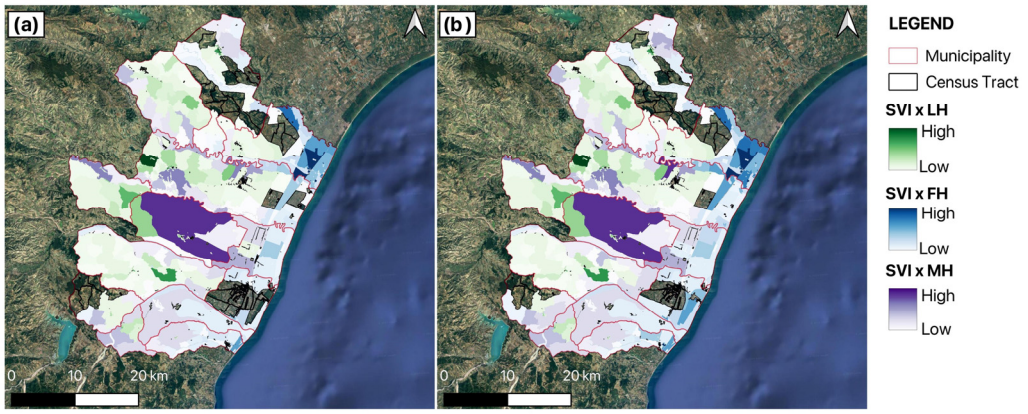

Figure 11. Spatial distribution of the census tracts based on the overlap between the SVI and landslide hazard (LH), the SVI and flood hazard (FH), and the SVI and multi-hazard (MH) events in different return period scenarios: 20–50 years (**a**), and 100–200 and 500 years (**b**). Basemap: Google Satellite.

Table 7. Final outcome of the integration of the SVI and FH, LH, and MH, with an indication of the number of census tracts in the different overlap classes for each municipality under investigation. The columns related to "LH Code", "FH Code", and "MH Code" show the type of hazard derived from the qualitative investigation (Table 2) for each semi-quantitative level. Each color represents the type of hazard considered in the integration process, whereas the shade represents the integration level. L = low; M = medium; H = high.

Municipality	Level	SVI x LH	LH Code	SVI x FH	FH Code	SVI x MH	MH Code
Bernalda	L	24	LH2, LH5, LH7, LH8, LH10, LH11	86	FH2, FH3	2	MH5, MH8
	M			4	FH2, FH3		
	H			15	FH2, FH3		
Colobraro	L	12	LH2, LH3, LH4, LH5, LH6, LH7, LH8, LH12	9	FH2, FH3	2	MH6, MH13
	M	1	LH12			6	MH3, MH7, MH9, MH10, MH13
Craco	L	18	LH2, LH3, LH5, LH7, LH10, LH12, LH13	7	FH3	4	MH5, MH9, MH11
	M	4	LH9, LH13			7	MH5, MH8, MH9
	H	1	LH4			2	MH11
Montalbano Jonico	L	15	LH2, LH4, LH5, LH8, LH12	11	FH2, FH3	3	MH5
	M	4	LH7, LH8, LH12			3	MH5, MH8, MH9
	H					1	MH14
Montescaglioso	L	34	LH3, LH4, LH5, LH8, LH9, LH12	26	FH2, FH3	3	MH4, MH7, MH12
	M	4	LH4, LH8			2	MH9, MH10
	H	8	LH4, LH9			1	MH14

Table 7. *Cont.*

Municipality	Level	SVI x LH	LH Code	SVI x FH	FH Code	SVI x MH	MH Code
Nova Siri	L	6	LH4, LH7, LH12	40	FH2, FH3	1	MH5
	M	2	LH7, LH8	3	FH2, FH3	2	MH9, MH13
	H			1	FH2		
Pisticci	L	59	LH1, LH2, LH4, LH5, LH8, LH13, LH11, LH12, LH13	77	FH2, FH3	17	MH5, MH8, MH14
	M	10	LH2, LH4, LH5, LH8, LH13	4	FH3	27	MH4, MH5, MH8
	H	4	LH4, LH5, LH8			2	MH5, MH14
Policoro	L			46	FH3		
	M			3	FH1, FH2, FH3		
Pomarico	L	30	LH2, LH4, LH5, LH7, LH10, LH11, LH12, LH13	17	FH3	19	MH11, MH13, MH14
	M	4	LH2, LH7, LH9			3	MH5, MH11, MH14
Rotondella	L	1	LH1	18	FH3	2	MH11, MH14
Tursi	L	29	LH2, LH4, LH5, LH6, LH7, LH10, LH12, LH13	19	FH3	8	MH1, MH5, MH8, MH12
	M	3	LH4, LH8, LH9			5	MH4, MH5, MH8
	H	1	LH2				
Valsinni	L	9	LH2, LH7, LH8, LH13,	8	FH2, FH3	2	MH7, MH10
	M	2	LH7, LH12			7	MH7, MH13, MH14
Scanzano Jonico	L			56	FH2, FH3	8	MH1, MH5, MH8, MH12
	M			1	FH3	3	MH5

Lastly, in order to present a detailed description of the overall results at the local level, Figures 12–14 depict a magnified view of the different study area sectors by integrating the outcomes derived from the overall quantitative analysis (Figure 11) with those from the hazard qualitative investigation (Figure 8). The codes represent the specific hazard (Table 1) to which the different levels of social vulnerability are exposed.

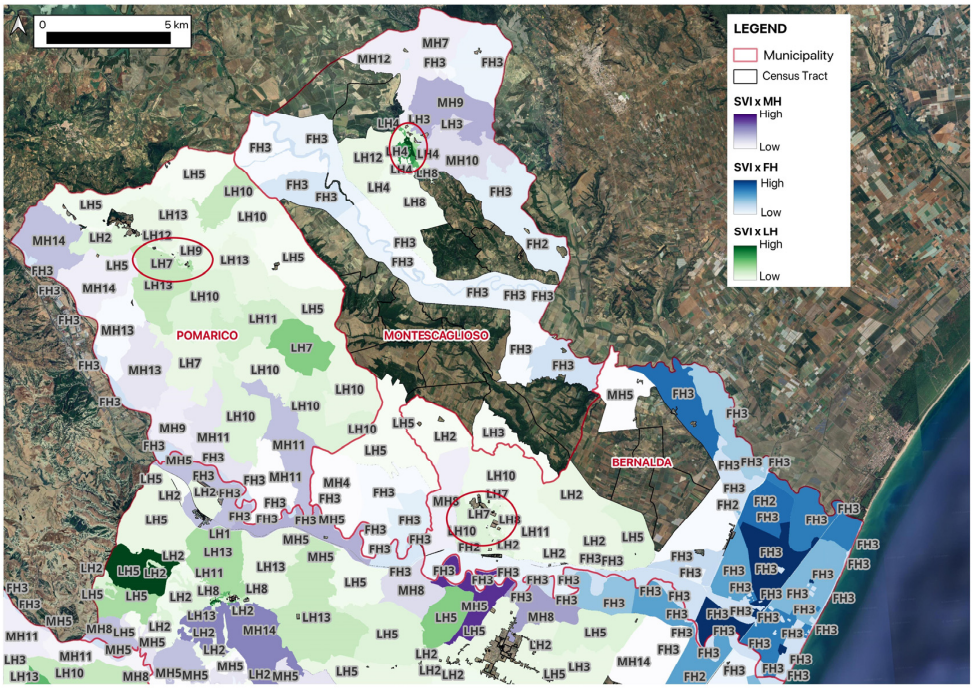

Figure 12. Spatial distribution of the different overlaps at the census tract level in the northern sector, with an indication of the specific hazard scenario derived from the hazard qualitative investigation. FH refers to the MPH scenario. The red circle represents the location of the town center. Basemap: Google Satellite.

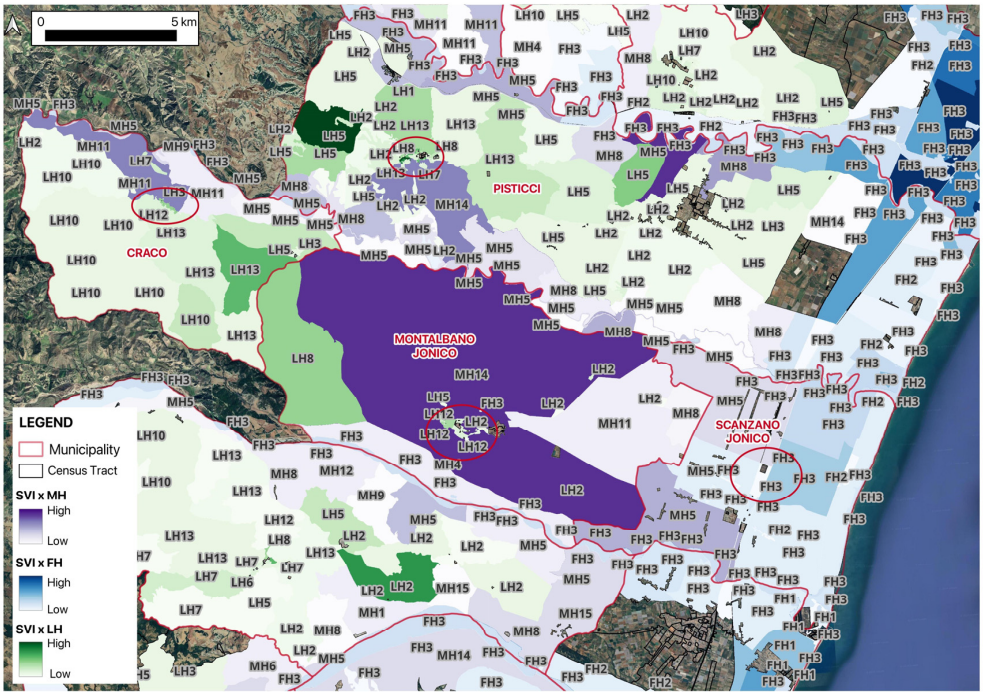

Figure 13. Spatial distribution of the different overlaps at the census tract level in the central sector, with an indication of the specific hazard scenario derived from the hazard qualitative investigation. FH refers to the MPH scenario. The red circle represents the location of the town center. Basemap: Google Satellite.

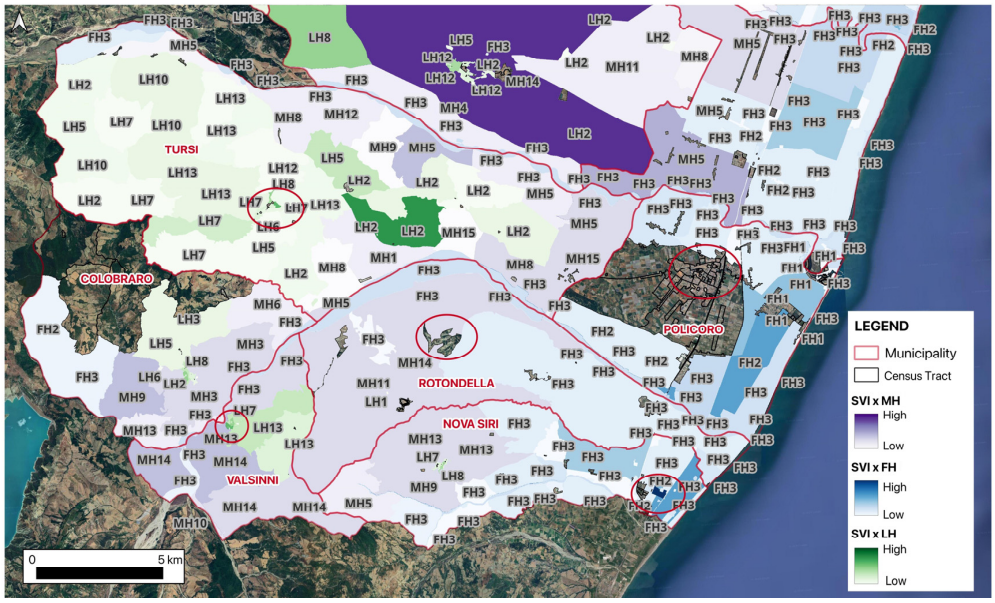

Figure 14. Spatial distribution of the different overlaps at the census tract level in the southern sector, with an indication of the specific hazard scenario derived from the hazard qualitative investigation. FH refers to the MPH scenario. The red circle represents the location of the town center. Basemap: Google Satellite.

4. Discussion and Conclusions

4.1. Integration Studies at the Sub-Municipality Level as a Tool for Emergency Planning

From a physical landscape perspective, the selection area (Section 3.1) falls in the marine terrace territory of the Basilicata Region [23], characterized by a variety of hazards and providing a multi-hazard hotspot for the application of methodological processes useful for risk management strategies. As shown from the main results, these hazards are spatially distributed as follows: Flood probability is mostly limited across census tracts located in the coastal zone and intersected by the main rivers (Bradano, Basento, Cavone, Agri, and Sinni). Census tracts influenced by landslide process and multi-hazard scenarios belong to landward municipalities. In particular, the most frequently occurring hazard scenarios related to the census tract investigated are LH2, FH2, and MH5. This implies that most of the census tracts intersected by single hazards correspond to areas classified as having a medium landslide hazard (P2) and areas that can be flooded due to flood events with a return period between 20 and 50 years (HPH), between 100 and 200 years (MPH), or exceeding 200 years (LPH). In terms of landslide hazards, our results confirm the outcomes linked to the Basilicata region, which is mostly characterized by having the highest percentage of the territory affected by medium landslide hazard [34]. Consequently, most of the census tracts belonging to MH5 scenarios are characterized by the coexistence of three main probabilities: P2 + HPH, P2 + MPH, and P2 + LPH (Section Multi-Hazard Context in the Basilicata Region). Considering the single-hazard context, the municipality of Bernalda shows the highest number of census tracts affected by flood hazards, while Craco, Montescaglioso, and Pisticci are mostly affected by landslide hazards. However, as shown in Section 3.2.2, Pisticci represents the highest multi-hazard hotspot at the sub-municipality level. Excluding the municipalities of Rotondella, Policoro, and Nova Siri, looking at the location of the city centers (Figures 12–14), the majority of them are limited in areas characterized by landslide hazard.

As regards social vulnerability, most of the census tracts fall in classes with very low social vulnerability. However, the majority of the municipalities are characterized by extended territories affected by medium, high, and very high social vulnerability, particularly in the city centers (Figure 9). This result is strictly correlated with the methodology used for the construction of the social vulnerability index. Firstly, the application of Equation (1)

(Section 2) on the socio-economic conditions of the Basilicata Region highlights the different contexts between rural/hilly areas, mostly characterized by classes with very low social vulnerability, and city centers, represented by higher-social-vulnerability classes, as the variables used have the highest values in the most populated areas, contributing to the composite index. Moreover, the city centers are characterized by higher census tract densities compared with those of rural areas, showing substantial differences in socio-economic features between these two areas.

Another consideration concerns the integration process (Sections 2 and 3.4), particularly the significance of the application of the risk formula (the product between hazard scenarios and social vulnerability). This study demonstrates the influence that the physical (hazard) and the socio-economic components have on each other in risk investigation. Examples are the census tracts located in the municipality of Bernalda and Montalbano Jonico. The former municipality is characterized by a high level of flood hazard and social vulnerability, resulting in higher classes of raster combination (Figure 12). The latter depicts census tracts affected by medium classes of multi-hazards and a high level of social vulnerability, leading to the higher exposure of this territory to hazards. Furthermore, the integration process applied in this work via the use of a cartographic approach conveys a clear spatial distribution of the socio-economic aspects based on the hazard exposure (Section 3.4). This could be a fundamental tool for emergency planning in the hands of civil protection that needs detailed information at the sub-municipality level. These final maps can let local authorities know the detailed risk context of their competence territories, and also allow them to construct plans capable of protecting the most vulnerable populations.

Looking at the general distribution of the multi-hazard context (Figure 11), the study area could be divided into three main areas based on the integration processes that highlight the type of vulnerability under different hazard scenarios. The population living along the Ionian coast is the most vulnerable to flood hazard scenarios, marking the first zone. Moving from the coast towards the northern direction, the second area is represented by inhabitants vulnerable to multi-hazards, followed by people vulnerable to landslide hazards.

In this respect, different risk management strategies can be implemented at the local level in order to reduce damages and impacts. The application of physical measures such as barriers, dikes, embankments for floods [56], or soil reinforcements and erosion-prevention strategies in the case of landslides [57] can also be supported by citizen participatory activities such as workshops, information campaigns, education courses, and strategic tools for disaster preparedness [58–60]. Considering Figure 11, these strategies can be implemented on the basis of the integration level between hazard and social vulnerability, considering only citizen science measures in areas characterized by low integration levels and including physical and non-physical strategies in the highest-risk areas. In both cases, the application of cost-based analyses or multicriteria investigations is highly recommended in order to provide monetary estimations and define various alternative strategies in different scenarios [61–63].

In addition, the present research points out a relevant outlook on the multidisciplinary methodologies that adopt the co-production of knowledge [64,65] and different techniques belonging to various study fields in order to promote risk reduction strategies. In this context, the use of "open-data" that can be accessed and re-used for research studies [66] is essential for accumulating knowledge and collecting information about the current state of our territories affected by any threats.

4.2. Limitations and Suggestions

The results of this study are strictly linked to the application of census tracts as a measure and geographic units. Although the use of this cartographic base is essential for research developed at the local level, many limitations need to be clarified. The census tracts show significant differences in terms of extension. Some of them limit inhabited centers, while others only cover portions of roads or special areas made up of particular

geomorphological entities, such as lakes, maritime islands, marshes or ponds, lagoons, fishing valleys, lakes, and uninhabited mountains [67]. As a consequence, relative or comparative analyses become complex within the same territory as the low frequency of census tracts falling in the same class would not correspond to low values of extension and therefore low exposure. In order to overcome this issue and to work on the same cartographically extended units, it would be useful to include grid cells of the same resolution [68–70]. Another limitation is the lack of open census data at the sub-municipality level. As shown in this research, only a few variables, that increment social vulnerability, were available from national datasets. Therefore, it is highly recommended that researchers provide and collect more socio-economic data for detailed vulnerability analyses, allowing the application of rigorous statistics, which form the basis of quantitative investigation. Another improvement, in terms of socio-economic features, could be the inclusion of land use data that can highlight the main characteristics of the territory exposed to hazards and that could help in the interpretation of the different types of vulnerability among the census tracts, as carried out in other studies conducted at the municipality level [71].

Concerning the development of this research, more effort should be put into hazard calculation. Results connected to flood return periods that range between 100 and 500 years could provide information about extreme events that have rarely occurred during human life. Indeed, one of the greatest challenges in risk studies is the understanding of the methods that are needed to combine periods related to natural and social processes. This is a key point in developing a climate change perspective that highlights the increase in the frequency and intensity of extreme events and will require high-resolution hazard assessments characterized by shorter return periods than those considered in the European Directive. As regards the landslide hazard assessment, a detailed susceptibility analysis could also be applied in risk analysis and integrated with social vulnerability [72,73]. In this context, physical vulnerability, related to the structural features of buildings and infrastructures, such as construction age, material, and the state maintenance of buildings, could be introduced as a development tool for landslide management strategies [74–76].

The last suggestion concerns the multi-hazard concept. In this study, we consider the coexistence of different hazards in the same territory. However, a challenging perspective would include the relationship between different hazards that provide more detailed information for multi-risk emergency planning. In this respect, improvements in quantitative correlations between multi-hazard scenarios could be achieved through stochastic, empirical, and mechanistic approaches [77]. This could help the scientific community and local authorities to increase their knowledge about multi-hazard contexts and implement adequate management strategies.

Author Contributions: Conceptualization, I.L.; investigation, I.L.; data curation, R.C.; writing—original draft preparation, I.L.; writing—review and editing, R.C. and A.R.; supervision, D.C. All authors have read and agreed to the published version of the manuscript.

Funding: This research was funded and carried out within the RETURN Extended Partnership project and received funding from European Union Next-GenerationEU (National Recovery and Resilience Plan—NRRP, Mission 4, Component 2, Investment 1.3—D.D. 1243 2/8/2022, PE0000005).

Institutional Review Board Statement: Not applicable.

Informed Consent Statement: Not applicable.

Data Availability Statement: The raw data supporting the conclusions of this article will be made available by the authors on request.

Acknowledgments: The authors would like to thank the anonymous reviewers for their valuable comments on this manuscript.

Conflicts of Interest: The authors declare no conflicts of interest.

References

1. UNDRR (United Nation Office for Disaster Risk Reduction). *Making Development Sustainable: The Future of Disaster Risk Management*; Global Assessment Report on Disaster Risk Reduction; United Nations: Geneva, Switzerland, 2015.
2. Clark, G.E.; Moser, S.C.; Ratick, S.J.; Dow, K.; Meyer, W.B.; Emani, S.; Jin, W.; Kasperson, J.X.; Kasperson, R.E.; Schwarz, H.E. Assessing the Vulnerability of Coastal Communities to Extreme Storms: The Case of Revere, MA, USA. *Mitig. Adapt. Strateg. Glob. Chang.* **1998**, *3*, 59–82. [CrossRef]
3. UNDRR. *Living with Risk: A Global Review of Disaster Reduction Initiatives*; 2004 Version; United Nations: New York, NY, USA, 2004.
4. UNISDR. *Terminology on Disaster Risk Reduction*; United Nations International Strategy for Disaster Reduction: Geneva, Switzerland, 2009.
5. UNDRR. Global Assessment Report on Disaster Risk Reduction 2022. In *Our World at Risk: Transforming Governance for a Resilient Future*; United Nations Office for Disaster Risk Reduction: Geneva, Switzerland, 2022.
6. Nguyen, H.D.; Dang, D.-K.; Bui, Q.-T.; Petrisor, A.-I. Multi-hazard Assessment Using Machine Learning and Remote Sensing in the North Central Region of Vietnam. *Trans. GIS* **2023**, *27*, 1614–1640. [CrossRef]
7. UNISDR. Flood Hazard and Risk Assessment 2017. In Words into Action Guidelines: National Disaster Risk Assessment Hazard Specific Risk Assessment. Available online: https://www.unisdr.org/files/52828_04floodhazardandriskassessment.pdf (accessed on 12 April 2024).
8. Varnes, D.; IAEG. *Landslide Hazard Zonation: A Review of Principles and Practice*; United Nations Scientific and Cultural Organization: Paris, France, 1984; pp. 1–6.
9. Versace, P.; Zuccaro, G.; Albarello, D.; Mugnozza, G.S. Natural and anthropogenic risks: Proposal for an interdisciplinary glossary. *Ital. J. Eng. Geol. Environ.* **2023**, *1*, 5–18. [CrossRef]
10. Field, C.B.; Barros, V.; Stocker, T.F.; Dahe, Q. (Eds.) *Managing the Risks of Extreme Events and Disasters to Advance Climate Change Adaptation: Special Report of the Intergovernmental Panel on Climate Change 2012*, 1st ed.; Cambridge University Press: Cambridge, UK, 2012. [CrossRef]
11. Drakes, O.; Tate, E. Social Vulnerability in a Multi-Hazard Context: A Systematic Review. *Environ. Res. Lett.* **2022**, *17*, 033001. [CrossRef]
12. Kalaycıoğlu, M.; Kalaycıoğlu, S.; Çelik, K.; Christie, R.; Filippi, M.E. An Analysis of Social Vulnerability in a Multi-Hazard Urban Context for Improving Disaster Risk Reduction Policies: The Case of Sancaktepe, İstanbul. *Int. J. Disaster Risk Reduct.* **2023**, *91*, 103679. [CrossRef]
13. Hejazi, S.J.; Sharifi, A.; Arvin, M. Assessment of Social Vulnerability in Areas Exposed to Multiple Hazards: A Case Study of the Khuzestan Province, Iran. *Int. J. Disaster Risk Reduct.* **2022**, *78*, 103127. [CrossRef]
14. Bixler, R.; Yang, P.E.; Richter, S.M.; Coudert, M. Boundary Crossing for Urban Community Resilience: A Social Vulnerability and Multi-Hazard Approach in Austin, Texas, USA. *Int. J. Disaster Risk Reduct.* **2021**, *66*, 102613. [CrossRef]
15. Pagliacci, F.; Russo, M. Be (and Have) Good Neighbours! Factors of Vulnerability in the Case of Multiple Hazards. *Ecol. Indic.* **2020**, *111*, 105969. [CrossRef]
16. Frigerio, I.; De Amicis, M. Mapping Social Vulnerability to Natural Hazards in Italy: A Suitable Tool for Risk Mitigation Strategies. *Environ. Sci. Policy* **2016**, *63*, 187–196. [CrossRef]
17. Guillard-Gonçalves, C.; Cutter, S.L.; Emrich, C.T.; Zêzere, J.L. Application of Social Vulnerability Index (SoVI) and Delineation of Natural Risk Zones in Greater Lisbon, Portugal. *J. Risk Res.* **2015**, *18*, 651–674. [CrossRef]
18. Rød, J.K.; Berthling, I.; Lein, H.; Lujala, P.; Vatne, G.; Bye, L.M. Integrated Vulnerability Mapping for Wards in Mid-Norway. *Local Environ.* **2012**, *17*, 695–716. [CrossRef]
19. Tate, E. Social Vulnerability Indices: A Comparative Assessment Using Uncertainty and Sensitivity Analysis. *Nat. Hazards* **2012**, *63*, 325–347. [CrossRef]
20. Lazzari, M.; Gioia, D.; Anzidei, B. Landslide Inventory of the Basilicata Region (Southern Italy). *J. Maps* **2018**, *14*, 348–356. [CrossRef]
21. Dal Sasso, S.F.; Manfreda, S.; Capparelli, G.; Versace, P.; Samela, C.; Spilotro, G.; Fiorentino, M. Hydrological and Geological Hazards in Basilicata. *L'Acqua* **2017**, *3*, 77–85. Available online: http://centrofunzionalebasilicata.it/it/pdf/2017_Dal_Sasso_et_al__L'Acqua%20n.%203_bassa.pdf (accessed on 4 April 2024).
22. Lazzari, M.; Piccarreta, M. Landslide Disasters Triggered by Extreme Rainfall Events: The Case of Montescaglioso (Basilicata, Southern Italy). *Geosciences* **2018**, *8*, 377. [CrossRef]
23. Schiattarella, M.; Giannandrea, P.; Corrado, G.; Gioia, D. Landscape Planning-Addressed Regional-Scale Mapping of Geolithological Units: An Example from Southern Italy. *J. Maps* **2024**, *20*, 2303335. [CrossRef]
24. Colacicco, R.; Refice, A.; Nutricato, R.; Bovenga, F.; Caporusso, G.; D'Addabbo, A.; La Salandra, M.; Lovergine, F.P.; Nitti, D.O.; Capolongo, D. High-Resolution Flood Monitoring Based on Advanced Statistical Modeling of Sentinel-1 Multi-Temporal Stacks. *Remote Sens.* **2024**, *16*, 294. [CrossRef]
25. Pellicani, R.; Argentiero, I.; Spilotro, G. GIS-Based Predictive Models for Regional-Scale Landslide Susceptibility Assessment and Risk Mapping along Road Corridors. *Geomat. Nat. Hazards Risk* **2017**, *8*, 1012–1033. [CrossRef]
26. Perrone, A.; Canora, F.; Calamita, G.; Bellanova, J.; Serlenga, V.; Panebianco, S.; Tragni, N.; Piscitelli, S.; Vignola, L.; Doglioni, A.; et al. A Multidisciplinary Approach for Landslide Residual Risk Assessment: The Pomarico Landslide (Basilicata Region, Southern Italy) Case Study. *Landslides* **2021**, *18*, 353–365. [CrossRef]

27. Greco, M.; Martino, G. Vulnerability Assessment for Preliminary Flood Risk Mapping and Management in Coastal Areas. *Nat. Hazards* **2016**, *82*, 7–26. [CrossRef]
28. De Musso, N.; Capolongo, D.; Refice, A.; Lovergine, F.P.; D'Addabbo, A.; Pennetta, L. Spatial Evolution of the December 2013 Metaponto Plain (Basilicata, Italy) Flood Event Using Multi-Source and High-Resolution Remotely Sensed Data. *J. Maps* **2018**, *14*, 219–229. [CrossRef]
29. Refice, A.; Capolongo, D.; Chini, M.; D'Addabbo, A. Improving Flood Detection and Monitoring through Remote Sensing. *Water* **2022**, *14*, 364. [CrossRef]
30. La Salandra, M.; Roseto, R.; Mele, D.; Dellino, P.; Capolongo, D. Probabilistic Hydro-Geomorphological Hazard Assessment Based on UAV-Derived High-Resolution Topographic Data: The Case of Basento River (Southern Italy). *Sci. Total Environ.* **2022**, *842*, 156736. [CrossRef]
31. Lapietra, I.; Rizzo, A.; Colacicco, R.; Dellino, P.; Capolongo, D. Evaluation of Social Vulnerability to Flood Hazard in Basilicata Region (Southern Italy). *Water* **2023**, *15*, 1175. [CrossRef]
32. Corbau, C.; Greco, M.; Martino, G.; Olivo, E.; Simeoni, U. Assessment of the Vulnerability of the Lucana Coastal Zones (South Italy) to Natural Hazards. *J. Mar. Sci. Eng.* **2022**, *10*, 888. [CrossRef]
33. La Salandra, M.; Colacicco, R.; Dellino, P.; Capolongo, D. An Effective Approach for Automatic River Features Extraction Using High-Resolution UAV Imagery. *Drones* **2023**, *7*, 70. [CrossRef]
34. ISPRA. *Landslides and Floods in Italy: Hazard and Risk Indicators—2021 Edition*; ISPRA: Rome, Italy, 2021; ISBN 978-88-448-1085-6.
35. Cutter, S.L.; Boruff, B.J.; Shirley, W.L. Social Vulnerability to Environmental Hazards. *Soc. Sci. Q.* **2003**, *84*, 242–261. [CrossRef]
36. Batabyal, S.; McCollum, M. Should Population Density Be Used to Rank Social Vulnerability in Disaster Preparedness Planning? *Econ. Model.* **2023**, *125*, 106165. [CrossRef]
37. Ehrlich, D.; Kemper, T.; Pesaresi, M.; Corbane, C. Built-up Area and Population Density: Two Essential Societal Variables to Address Climate Hazard Impact. *Environ. Sci. Policy* **2018**, *90*, 73–82. [CrossRef]
38. Frigerio, I.; Ventura, S.; Strigaro, D.; Mattavelli, M.; De Amicis, M.; Mugnano, S.; Boffi, M. A GIS-Based Approach to Identify the Spatial Variability of Social Vulnerability to Seismic Hazard in Italy. *Appl. Geogr.* **2016**, *74*, 12–22. [CrossRef]
39. Holand, I.S.; Lujala, P.; Rød, J.K. Social Vulnerability Assessment for Norway: A Quantitative Approach. *Nor. Geogr. Tidsskr. Nor. J. Geogr.* **2011**, *65*, 1–17. [CrossRef]
40. Holand, I.S.; Lujala, P. Replicating and Adapting an Index of Social Vulnerability to a New Context: A Comparison Study for Norway. *Prof. Geogr.* **2013**, *65*, 312–328. [CrossRef]
41. Martins, V.N.; Sousa, E.; Silva, D.; Cabral, P. Social Vulnerability Assessment to Seismic Risk Using Multicriteria Analysis: The Case Study of Vila Franca Do Campo (São Miguel Island, Azores, Portugal). *Nat. Hazards* **2012**, *62*, 385–404. [CrossRef]
42. Von Szombathely, M.; Hanf, F.S.; Bareis, J.; Meier, L.; Oßenbrügge, J.; Pohl, T. An Index-Based Approach to Assess Social Vulnerability for Hamburg, Germany. *Int. J. Disaster Risk Sci.* **2023**, *14*, 782–794. [CrossRef]
43. Chakraborty, J.; Graham, A.T.; Burrell, E.M. Population Evacuation: Assessing Spatial Variability in Geophysical Risk and Social Vulnerability to Natural Hazards. *Nat. Hazards Rev.* **2005**, *6*, 23–33. [CrossRef]
44. Rana, S.; Dharanirajan, K.T.J.; Mandal, K.K. Assessment of Social Vulnerability of Landslides in the Darjeeling District Using MCDA-Based GIS Techniques. *Disaster Adv.* **2022**, *15*, 8–15. [CrossRef]
45. Lee, Y.-J. Social Vulnerability Indicators as a Sustainable Planning Tool. *Environ. Impact Assess. Rev.* **2014**, *44*, 31–42. [CrossRef]
46. Cutter, S.L.; Barnes, L.; Berry, M.; Burton, C.; Evans, E.; Tate, E.; Webb, J. A Place-Based Model for Understanding Community Resilience to Natural Disasters. *Glob. Environ. Chang.* **2008**, *18*, 598–606. [CrossRef]
47. De Loyola Hummell, B.M.; Cutter, S.L.; Emrich, C.T. Social Vulnerability to Natural Hazards in Brazil. *Int. J. Disaster Risk Sci.* **2016**, *7*, 111–122. [CrossRef]
48. Yi, L.; Zhang, X.; Ge, L.; Zhao, D. Analysis of Social Vulnerability to Hazards in China. *Environ. Earth Sci.* **2014**, *71*, 3109–3117. [CrossRef]
49. Armaş, I. Multi-Criteria Vulnerability Analysis to Earthquake Hazard of Bucharest, Romania. *Nat. Hazards* **2012**, *63*, 1129–1156. [CrossRef]
50. Flanagan, B.E.; Gregory, E.W.; Hallisey, E.J.; Heitgerd, J.L.; Lewis, B.A. Social Vulnerability Index for Disaster Management. *J. Homel. Secur. Emerg. Manag.* **2011**, *8*, 00010220215477355179 2. [CrossRef]
51. Fekete, A. Validation of a Social Vulnerability Index in Context to River-Floods in Germany. *Nat. Hazards Earth Syst. Sci.* **2009**, *9*, 393–403. [CrossRef]
52. Schmidtlein, M.C.; Deutsch, R.C.; Piegorsch, W.W.; Cutter, S.L. A Sensitivity Analysis of the Social Vulnerability Index. *Risk Anal.* **2008**, *28*, 1099–1114. [CrossRef] [PubMed]
53. Chen, W.; Cutter, S.L.; Emrich, C.T.; Shi, P. Measuring Social Vulnerability to Natural Hazards in the Yangtze River Delta Region, China. *Int. J. Disaster Risk Sci.* **2013**, *4*, 169–181. [CrossRef]
54. Tasnuva, A.; Hossain, M.R.; Salam, R.; Islam AR, M.T.; Patwary, M.M.; Ibrahim, S.M. Employing Social Vulnerability Index to Assess Household Social Vulnerability of Natural Hazards: An Evidence from Southwest Coastal Bangladesh. *Environ. Dev. Sustain.* **2021**, *23*, 10223–10245. [CrossRef]
55. Fatemi, F.; Ardalan, A.; Aguirre, B.; Mansouri, N.; Mohammadfam, I. Social Vulnerability Indicators in Disasters: Findings from a Systematic Review. *Int. J. Disaster Risk Reduct.* **2017**, *22*, 219–227. [CrossRef]

56. Goltermann, D.; Marengwa, J. SAWA Final Report Summary, Hamburg. 2012. Available online: http://archive.northsearegion.eu/files/repository/20130814132256_SAWA_Final_Report_Summary.pdf (accessed on 22 May 2024).
57. Andersson-Sköld, Y.; Lars, N. Effective and sustainable flood and landslide risk reduction measures: An investigation of two assessment frameworks. *Int. J. Disaster Risk Sci.* **2016**, *7*, 374–392. [CrossRef]
58. Ramesh, M.V.; Thirugnanam, H.; Mohanan, N.K.; Singh, B.; Ekkirala, H.C.; Guntha, R. Community Scale Landslide Resilience: A Citizen-Science Approach. In *Progress in Landslide Research and Technology 2023*; Alcántara-Ayala, I., Arbanas, Z., Huntley, D., Konagi, K., Arbanas, S.M., Mikš, S., Ramesh, M.V., Sassa, S., Eds.; Springer: Cham, Switzerland, 2023; Volume 2, Issue 2. [CrossRef]
59. Kocaman, S.; Anbaroglu, B.; Gokceoglu, C.; Altan, O. A review on citizen science (CitSci) applications for disaster management. *Int. Arch. Photogramm. Remote Sens. Spat. Inf. Sci.* **2018**, *42*, 301–306. [CrossRef]
60. Paul, J.D.; Buytaert, W.; Allen, S.; Ballesteros-Cánovas, J.A.; Bhusal, J.; Cieslik, K.; Supper, R. Citizen Science for Hydrological Risk Reduction and Resilience Building. *Wiley Interdiscip. Rev. Water* **2018**, *5*, e1262. [CrossRef]
61. Mechler, R.; Czajkowski, J.; Kunreuther, H.; Michel-Kerjan, E.; Botzen, W.; Keating, A.; McQuistan, C.; Cooper, N.; O'Donnell, I. Making Communities More Flood Resilient: The Role of Cost Benefit Analysis and Other Decision-Support Tools in Disaster Risk Reduction 2014. Available online: https://pure.iiasa.ac.at/id/eprint/11193/1/Mechler%20et%20al%20White%20paper%20Making%20communities%20more%20flood%20resilient%20-%20the%20role%20of%20cost-benefit%20analysis%20and%20other%20decision-support%20tools%202015.pdf (accessed on 21 May 2024).
62. Galve, J.P.; Cevasco, A.; Brandolini, P.; Piacentini, D.; Azañón, J.M.; Notti, D.; Soldati, M. Cost-based analysis of mitigation measures for shallow-landslide risk reduction strategies. *Eng. Geol.* **2016**, *213*, 142–157. [CrossRef]
63. Lyu, H.-M.; Yin, Z.-Y. An improved MCDM combined with GIS for risk assessment of multi-hazards in Hong Kong. *Sustain. Cities Soc.* **2023**, *91*, 104427. [CrossRef]
64. Righi, E.; Lauriola, P.; Ghinoi, A.; Giovannetti, E.; Soldati, M. Disaster Risk Reduction and Interdisciplinary Education and Training. *Prog. Disaster Sci.* **2021**, *10*, 100165. [CrossRef]
65. Lahiri, S.; Snowden, B.; Gu, J.; Krishnan, N.; Yellin, H.; Ndiaye, K. Multidisciplinary Team Processes Parallel Natural Disaster Preparedness and Response: A Qualitative Case Study. *Int. J. Disaster Risk Reduct.* **2021**, *61*, 102369. [CrossRef]
66. Murray-Rust, P. Open Data in Science. *Nat. Preced.* **2008**. [CrossRef]
67. Istat. Atti del 9° Censimento Generale Dell'industria e dei servizi e Censimento Delle Istituzioni Non Prot. Le Sezioni di Censimento 2016. Available online: https://www.istat.it/it/files//2016/02/Atti-CIS_Fascicolo_5.pdf (accessed on 12 April 2024).
68. Raduszynski, T.; Numada, M. Measure and Spatial Identification of Social Vulnerability, Exposure and Risk to Natural Hazards in Japan Using Open Data. *Sci. Rep.* **2023**, *13*, 664. [CrossRef] [PubMed]
69. Karanja, J.; Lawrence, M.K. Scale Implications and Evolution of a Social Vulnerability Index in Atlanta, Georgia, USA. *Nat. Hazards* **2022**, *113*, 789–812. [CrossRef]
70. Tate, E.; Rahman, M.d.A.; Emrich, C.T.; Sampson, C.C. Flood Exposure and Social Vulnerability in the United States. *Nat. Hazards* **2021**, *106*, 435–457. [CrossRef]
71. Lapietra, I.; Colacicco, R.; Capolongo, D.; La Salandra, M.; Rinaldi, A.; Dellino, P. Unveiling Social Vulnerability to Natural Hazards in the EEA and UK: A Systematic Review with Insights for Enhanced Emergency Planning and Risk Reduction. *Int. J. Disaster Risk Reduct.* **2024**, *108*, 104507. [CrossRef]
72. Rizzo, A.; Vandelli, V.; Buhagiar, G.; Micallef, A.S.; Soldati, M. Coastal Vulnerability Assessment along the North-Eastern Sector of Gozo Island (Malta, Mediterranean Sea). *Water* **2020**, *12*, 1405. [CrossRef]
73. Batista, E.F.; De Brum Passini, L. Development and Application of a Social Vulnerability Index (SOVI) to Landslide Risk Analysis in Ribeira Medium Valley, Brazil. *Obs. Econ. Latinoam.* **2023**, *21*, 2801–2829. [CrossRef]
74. Guillard-Gonçalves, C.; Zêzere, J. Combining Social Vulnerability and Physical Vulnerability to Analyse Landslide Risk at the Municipal Scale. *Geosciences* **2018**, *8*, 294. [CrossRef]
75. Bera, S.; Balamurugan, G.; Oommen, T. Indicator-Based Approach for Assigning Physical Vulnerability of the Houses to Landslide Hazard in the Himalayan Region of India. *Int. J. Disaster Risk Reduct.* **2020**, *50*, 101891. [CrossRef]
76. Chen, Q.; Chen, L.; Gui, L.; Yin, K.; Shrestha, D.P.; Du, J.; Cao, X. Assessment of the Physical Vulnerability of Buildings Affected by Slow-Moving Landslides. *Nat. Hazards Earth Syst. Sci.* **2020**, *20*, 2547–2565. [CrossRef]
77. Tilloy, A.; Malamud, B.D.; Winter, H.; Joly-Laugel, A. A review of quantification methodologies for multi-hazard interrelationships. *Earth-Sci. Rev.* **2019**, *196*, 102881. [CrossRef]